

Passivation of organic light emitting diodes with $\text{Al}_2\text{O}_3/\text{Ag}/\text{Al}_2\text{O}_3$ multilayer thin films grown by twin target sputtering system

Jin-A Jeong and Han-Ki Kim*

Department of Information and Nano-Materials Engineering, Kumoh National Institute of Technology, 1 Yangho-dong, Gumi, Gyeongbuk 730-701, Korea
TEL:+82-54-478-7746, e-mail:hkkim@kumoh.ac.kr

Keywords : OLED, $\text{Al}_2\text{O}_3/\text{Ag}/\text{Al}_2\text{O}_3$, Passivation, Surface Plasmon Resonance (SPR)

Abstract

The characteristics of $\text{Al}_2\text{O}_3/\text{Ag}/\text{Al}_2\text{O}_3$ multilayer passivation prepared by twin target sputtering (TTS) system for organic light emitting diodes. The $\text{Al}_2\text{O}_3/\text{Ag}/\text{Al}_2\text{O}_3$ multilayer thin film passivation on a PET substrate had a high transmittance of 86.44 % and low water vapor transmission rate (WVTR) of 0.011 $\text{g}/\text{m}^2\text{-day}$ due to the surface plasmon resonance (SPR) effect of Ag interlayer and effective multilayer structure for preventing the intrusion of water vapor. Using synchrotron x-ray scattering and field emission scanning electron microscope (FESEM) examinations, we investigated the growth behavior of Ag layer on the Al_2O_3 layer to explain the SPR effect of the Ag layer. This indicates that an $\text{Al}_2\text{O}_3/\text{Ag}/\text{Al}_2\text{O}_3$ multilayer passivation is a promising thin film passivation scheme for organic based flexible optoelectronics.

1. Introduction

Recently the organic based flexible optoelectronics such as flexible organic light emitting diodes (OLEDs), flexible organic photovoltaic (OPVs) and flexible organic thin film transistors (OTFTs) gain a considerable interest due to their lightweight, robust profile, their ability to flex, curve, roll and fold for portability, and engineering design freedom afford by these characteristics [1-3]. However, the long-term stability of flexible optoelectronics is still limited due to the instability of the organic materials, which easily react with oxygen and moisture in the air [4]. Although the lid type encapsulation could be employed in the OLEDs or OPVs fabricated on the glass substrate, the use of lid type encapsulation on the flexible polymer substrate is difficult due to the rigidity of glass or metal encapsulation. For those reasons, transparent SiN_x , SiO_x , SiO_xN_y , AlO_x , and $\text{Al}_2\text{O}_3:\text{N}$ films have been currently employed as

flexible thin film passivation for OLEDs or OPVs [5]. However, a single inorganic thin film is not sufficiently dense to protect flexible optoelectronic devices from permeation by moisture and oxygen and not appropriate to apply flexible substrate. Therefore, alternating organic-inorganic (Barix coating) multilayers have been proposed to achieve ultra high barrier properties. However, dielectric/metal/dielectric multilayer passivation simultaneously using the advantages of the metal layer such as ductility and surface plasmon resonance (SPR) is not suggested so far as a flexible thin film passivation [6].

In this work, we report on the characteristics of an aluminum oxide (Al_2O_3)/Ag/ Al_2O_3 multilayer passivation grown on a polyethylene terephthalate (PET) substrate and describe the effect of surface plasmon resonance in the Ag layer on the optical properties of the flexible $\text{Al}_2\text{O}_3/\text{Ag}/\text{Al}_2\text{O}_3$ multilayer passivation.

2. Experimental

To realize direct passivation sputtering on the organic layers, we developed a specially designed TTS system with linear gun consisting of ladder type magnet array [5]. Figure 1 shows a schematic diagram of the system and picture of the plasma uniformly confined between two Al targets. The TTS system was characterized by ladder type magnet array and position of facing Al target planes generating closed magnet flux from the N-pole to the S-pole as shown in Fig. 1(a). Therefore, most the energetic particles, such as charged ions and γ -electrons resulting in the optical and electrical degradation of organic films, could be effectively confined between the Al targets. Effectively confined plasma between Al targets was shown in Fig. 1(b). It was shown that the substrate

was not directly affected by irradiation of plasma due to geometry of twin Al targets and confined plasma. In addition, symmetrically arranged two Al target planes could form high-density plasma between Al targets. After the deposition of the bottom Al₂O₃ film, a Ag layer was deposited onto the Al₂O₃ film by thermal evaporation at a constant deposition rate of 0.02 nm/sec as a function of thickness (2~20 nm). Subsequently, the 70 nm-thick top Al₂O₃ film was deposited onto the Ag layer under deposition conditions identical to those for the bottom Al₂O₃ film.

The transmittance of the flexible Al₂O₃/Ag/Al₂O₃ multilayer passivation was measured in a wavelength range from 220 to 800 nm using a UV/visible spectrometer. The WVTR value for Al₂O₃/Ag/Al₂O₃ films grown on PET substrates (5 cm × 5 cm) was determined at 38±2 °C, 100 % R. H. with a MOCON tester for 72 hours.

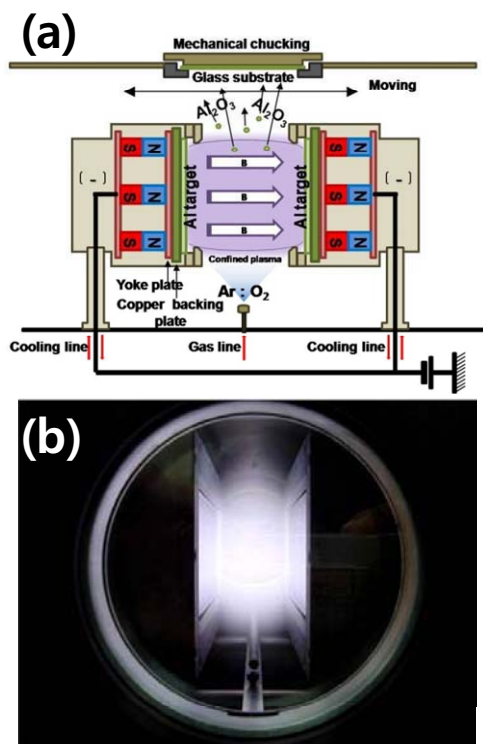


Fig. 1. (a) Schematic diagram of specially designed twin target sputter (TTS) system and (b) picture of effectively confined plasma between Al targets.

In addition, the shape and surface morphology of the Ag layer at the interface with the bottom Al₂O₃ film were analyzed as a function of Ag thickness using a FESEM (JSM-6500F). Finally, the growth behavior of the Ag layer on the Al₂O₃ film was

examined by synchrotron x-ray scattering as the thickness of the Ag layer increased. The synchrotron X-ray scattering measurements were carried out at the 5C2 GIST beam line at Pohang Light Source (PLS) in Korea. The wavelength of the incident X-rays was set at 1.243 Å by a double bounce Si(111) monochromator.

3. Results and discussion

Figure 2 shows the dependence of discharge voltage on the working pressure. It shows that as the

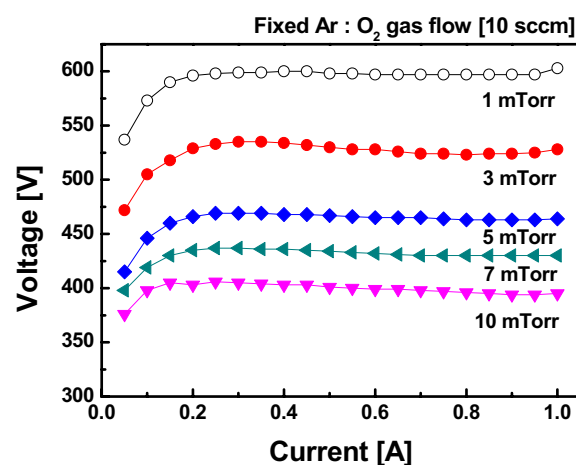


Fig. 2. Discharge voltage and current of TTS system with increasing power and working pressure at constant Ar flow rate

working pressure increases, the discharge voltage decreases. By increasing working pressure from 1 to 10 mTorr, we can simply decrease the discharge voltage from 600 to 400 V, which is one of the key parameters in a plasma damage free sputtering. The decrease of the discharge voltage could be attributed to the increased amount of ionized ions and high energy γ -electrons. However, the discharge voltage was kept constantly at constant working pressure with increasing input powers. The stable discharge voltage indicates that the TTS technique is stable plasma process for deposition of Al₂O₃/Ag/Al₂O₃ passivation on organic layers.

Figure 3 shows the optical transmittance and WVTR of the Al₂O₃/Ag/Al₂O₃ multilayer grown on a PET substrate and glass substrate as a function of Ag thickness with inset of the transparent and flexible Al₂O₃/Ag(10 nm)/Al₂O₃ multilayer picture.

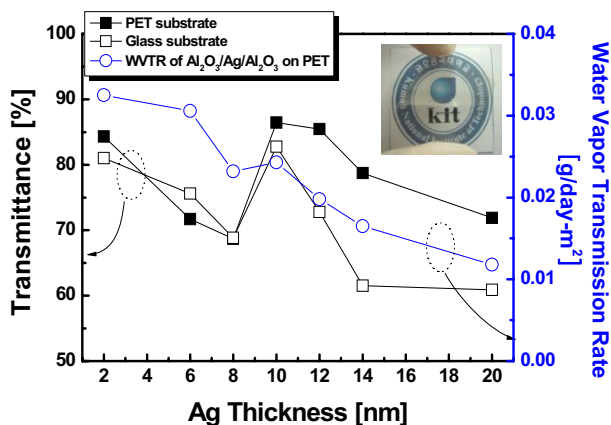


Fig. 3. Transmittance at 550 nm wavelength and water vapor transmission rate of $\text{Al}_2\text{O}_3/\text{Ag}/\text{Al}_2\text{O}_3$

It was shown that $\text{Al}_2\text{O}_3/\text{Ag}/\text{Al}_2\text{O}_3$ multilayer at an Ag thickness of 2~8 nm shows a fairly low optical transmittance regardless of substrates due to the absorption of aggregated Ag islands. However, both $\text{Al}_2\text{O}_3/\text{Ag}/\text{Al}_2\text{O}_3$ multilayer with an Ag thickness of 10 nm fabricated on PET and glass substrate shows the highest optical transmittance of 86.44 and 82.76 % respectively due to the SPR effect of the Ag interlayer. It has been reported that the high index of refraction contrast between Ag and the dielectric layer results in efficient plasmon coupling such that visible transparency greater than 90 % can be achieved. Therefore, the dramatically increased transmittance in both $\text{Al}_2\text{O}_3/\text{Ag}/\text{Al}_2\text{O}_3$ multilayer fabricated on a PET and glass substrates with an Ag thickness of 10 nm can be attributed to effective SPR phenomenon of a Ag interlayer sandwiched by the Al_2O_3 layers. However, further increase of Ag thickness resulted in a decrease of transmittance due to absorption of the Ag interlayer even though it had the better flexibility.

The WVTR value of the $\text{Al}_2\text{O}_3/\text{Ag}/\text{Al}_2\text{O}_3$ multilayer also depends on the thickness of Ag interlayer. As increasing Ag thickness in the $\text{Al}_2\text{O}_3/\text{Ag}/\text{Al}_2\text{O}_3$ multilayer, the WVTR value monotonically decreased because the thicker Ag layer could effectively prevent the intrusion of the water vapor. Despite of very thin thickness of the $\text{Al}_2\text{O}_3/\text{Ag}/\text{Al}_2\text{O}_3$ multilayer, the WVTR of the multilayer passivation shows the lowest WVTR value 0.011 $\text{g}/\text{m}^2\text{-day}$ at the Ag thickness of 20 nm.

Figure 4 shows the surface FESEM images of the Ag interlayer grown on the Al_2O_3 layer with an increase in the thickness of Ag layer. It was found that the morphology and shape of the Ag layer were

critically dependent on the Ag thickness. In case of 2 nm thick Ag layer in Fig. 4(a), it shows disconnected Ag islands corresponds to light absorption in the $\text{Al}_2\text{O}_3/\text{Ag}(2\text{nm})/\text{Al}_2\text{O}_3$ multilayer. The 8 nm thick Ag layer on the Al_2O_3 film in Fig. 4(b) shows randomly connected Ag channels. Fairly high WVTR value and low transmittance of the $\text{Al}_2\text{O}_3/\text{Ag}/\text{Al}_2\text{O}_3$ multilayer with 2~8 nm Ag thickness could be attributed to the disconnected Ag interlayer which act as the path of water vapor and source of light absorption. However, in the case of 10 nm-thick Ag film shown in Fig. 4(c), the Ag layer was continuous. The high transmittance of the $\text{Al}_2\text{O}_3/\text{Ag}/\text{Al}_2\text{O}_3$ multilayer with Ag thickness of 10 nm could be attributed to the fact that the effective SPR of the Ag layer occurred in the transition region from an aggregated Ag layer to a continuous Ag layer. It was reported that the critical thickness of the Ag layer for transition from distinct islands to a continuous film is predominantly between 10 and 20 nm.

To investigate the growth behavior of the Ag layer on the Al_2O_3 film in detail, we employed synchrotron x-ray scattering. Because the x-ray refraction of the Ag layer is heavily influenced by the rough surface morphology of the PET substrate, we also prepared a $\text{Al}_2\text{O}_3/\text{Ag}/\text{Al}_2\text{O}_3$ multilayer on a glass substrate under growth conditions identical to those of the $\text{Al}_2\text{O}_3/\text{Ag}/\text{Al}_2\text{O}_3$ multilayer grown on the PET substrate. Figure 5 shows the x-ray refractivity curve of the Ag layer as a function of increasing Ag thickness. From the period of the oscillations, ΔQ_z , one can easily estimate the thickness of Ag layer, which is given by $2\pi/\Delta Q_z$. In case of the 2 nm Ag layer, there is a well-defined small intensity oscillation that gives the Al_2O_3 thickness (~ 70 nm).

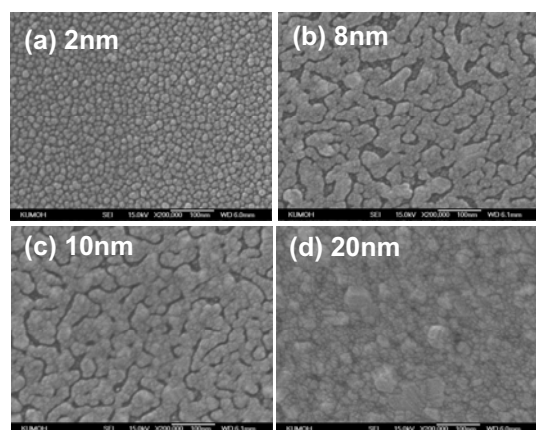


Fig. 4. Surface FESEM images of Ag layer deposited on the bottom Al_2O_3 film

At an Ag thickness above 8 nm, the broad oscillation intensity indicates the formation of a thin Ag layer. As the thickness of Ag layer increases, the oscillation period (ΔQ_z) decreases.

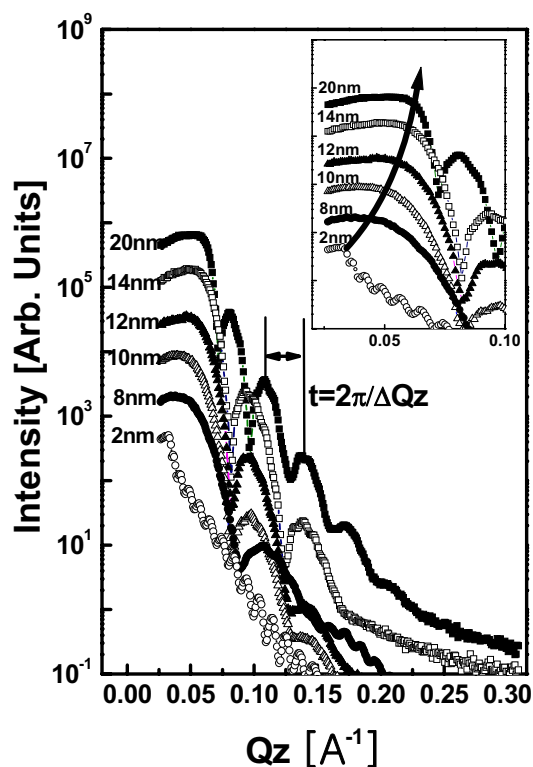


Fig. 5. The X-ray refractivity curves show regular intensity oscillations with increasing Ag thickness. The inset shows the x-ray refractivity curve near the critical angle.

The inset of Figure 5 shows the x-ray reflectivity near the critical angle. As the Ag layer thickness increase, the critical angle of the Ag layer shifts to the right due to the change in the electron density in the Ag layer, which is critically affected by the shape of the Ag layer. Because the 2 nm-thick Ag layer is made up of disconnected Ag islands, as seen in Fig. 4(a), the 2 nm Ag film has a low electron density. Therefore, the sample exhibits the lowest critical angle. The shift of the critical angle with increasing Ag thickness indicates a change in the electron density in the Ag layer caused by the transition of the Ag layer shape from disconnected islands to a continuous Ag film. The sample with the 10 nm-thick Ag layer, which is the optimized condition for SPR, has a higher critical angle than those with 2 and 8 nm-thick Ag layers, due to a higher electron density in the Ag layer. This

indicates that 10 nm-thick Ag layer is in the transition region from an island Ag layer, i.e. a disconnected layer, to a completely connected film. In addition, the Yoneda wing positions were moved into specular peak with an increase in the thickness of the Ag layer.

4. Summary

The $\text{Al}_2\text{O}_3/\text{Ag}/\text{Al}_2\text{O}_3$ multilayer thin film passivation on the PET substrate has a high transmittance of 86.44 % and low WVTR due to the SPR effects of the Ag interlayer and the effective multilayer structure that prevents the intrusion of water vapor. An Ag metal layer with a critical thickness of 10 nm sandwiched between two Al_2O_3 layers was shown to provide significantly improved transmittance and mechanical robustness upon substrate bending due to the SPR effects and the ductility of Ag layer. This indicates that $\text{Al}_2\text{O}_3/\text{Ag}/\text{Al}_2\text{O}_3$ multilayer passivation is a promising thin film passivation scheme for organic-based flexible optoelectronics.

5. References

1. Y. Li, L.-W. Tan, X.-T. Hao, K. S. Ong, F. Zhu, and L. -S. Hung, *Appl. Phys. Lett.* **86**, 153508 (2005).
2. C. J. Brabec, N. S. Sariciftci, and J. J. Hummelen, *Adv. Funct. Mater.* **11**, 15 (2001).
3. A. L. Briseno, R. J. Tseng, M.-M. Ling, E. H. L. Falcao, Y. Yang, F. Wudl, and Z. Bao, *Adv. Mater.* **18**, 2320 (2006).
4. M. Schaer, F. Nuesch, D. Berner, W. Leo, and L. Zuppiroli, *Adv. Funct. Mater.* **11**, 116 (2001).
5. J.-M. Moon and H.-K. Kim, *J. Electrochem. Soc.* **155**, J187 (2008).
6. Jin-A Jeong, Han-Ki Kim and Min-Su Yi, *Appl. Phys. Lett.* **93**, 0333501 (2008).